

## Plasma texturing of multicrystalline silicon for solar cell using remote-type pin-to-plate dielectric barrier discharge

This article has been downloaded from IOPscience. Please scroll down to see the full text article.

2009 J. Phys. D: Appl. Phys. 42 215201

(<http://iopscience.iop.org/0022-3727/42/21/215201>)

View [the table of contents for this issue](#), or go to the [journal homepage](#) for more

Download details:

IP Address: 115.145.196.96

The article was downloaded on 29/05/2013 at 12:59

Please note that [terms and conditions apply](#).

# Plasma texturing of multicrystalline silicon for solar cell using remote-type pin-to-plate dielectric barrier discharge

Jae Beom Park<sup>1</sup>, Jong Sik Oh, Elly Gil, Se-Jin Kyoung<sup>2</sup>, Jung-Sik Kim<sup>3</sup>  
and Geun Young Yeom<sup>1,2,4,5</sup>

<sup>1</sup> SKKU Advanced Institute of Nano Technology (SAINT), Sungkyunkwan University, Suwon, Kyunggi-do 440-746, South Korea

<sup>2</sup> Department of Advanced Materials Engineering, Sungkyunkwan University, Suwon, Kyunggi-do 440-746, South Korea

<sup>3</sup> JUSUNG Eng. Neungpyeong-ri, Opo-eup, Gwangju-si, Gyeonggi-do, South Korea

<sup>4</sup> National Program for Tera-Level Nanodevice, Hawolgok-dong, Sungbuk-ku, Seoul 136-791, South Korea

E-mail: [gyeom@skku.edu](mailto:gyeom@skku.edu)

Received 23 June 2009, in final form 19 August 2009

Published 6 October 2009

Online at [stacks.iop.org/JPhysD/42/215201](http://stacks.iop.org/JPhysD/42/215201)

## Abstract

Multicrystalline silicon (mc-Si) was etched using a pin-to-plate-type remote dielectric barrier discharge, and the effect of adding  $\text{NF}_3$  to  $\text{N}_2$  (40 slm) and  $\text{O}_2$  to  $\text{N}_2$  (40 slm)/ $\text{NF}_3$  (1 slm) on the characteristics of mc-Si etching and texturing was investigated. The addition of  $\text{NF}_3$  at flow rates up to that of  $\text{N}_2$  increased the mc-Si etch rate continuously by increasing the number of F radicals in the gas mixture. Furthermore, the addition of  $\text{O}_2$  at flow rates of up to 400 sccm to  $\text{N}_2$  (40 slm)/ $\text{NF}_3$  (1 slm) further increased the mc-Si etch rate by more than two times (749.6 nm/scan,  $0.25 \text{ m min}^{-1}$ ), as compared with that without oxygen by the further dissociation of  $\text{NF}_3$  caused by oxygen. In particular, the addition of  $\text{O}_2$  to  $\text{N}_2/\text{NF}_3$  increased the surface roughness, due to the micromasking (local surface oxidation) effect and, by adding 600 sccm  $\text{O}_2$ , a reflectance of 20–30% in the visible wavelength could be obtained due to the formation of optimal wave-type surface morphology.

## 1. Introduction

Multicrystalline silicon (mc-Si) solar cells have been extensively studied and used in a variety of commercial photovoltaic products. The interest in this material is due to its abundance and to the ease with which it can be adapted to the current technology developed for silicon integrated circuit fabrication. Furthermore, mc-Si solar cells have been shown to have a high energy conversion efficiency, which is just a little lower than that achieved with single-crystalline silicon [1], while fabrication that uses a sliced mc-Si ingot as the substrate is much less expensive than that from single-crystal silicon.

During the preparation of mc-Si wafers, the mechanical saw damage caused by the slicing of the mc-Si ingots into wafers with a wire saw leads to the formation of micro-cracks

and a strained layer. These defects are known to degrade the solar cell performance, so a saw damage removal process (etching) is generally performed [2]. The front surface of the mc-Si substrate is normally textured at the same time as the saw damage etch processing. This texturing of the mc-Si surface is done in order to increase the efficiency of the solar cell by reducing the light reflection from its surface and by increasing the scattering angle for effective light absorption in the bulk material [3].

Various techniques for the etching and texturing of the mc-Si substrates have been investigated. Currently, isotropic wet processing with an alkaline or acid solution [4, 5] is the treatment of choice for commercial products. However, wet-chemical anisotropic etching tends to form random pyramids with an exclusively  $\langle 100 \rangle$  crystal orientation, and so can cause unwanted steps or crevices between the grains of the mc-Si substrate. Furthermore, wet treatments are environmentally

<sup>5</sup> Author to whom any correspondence should be addressed.

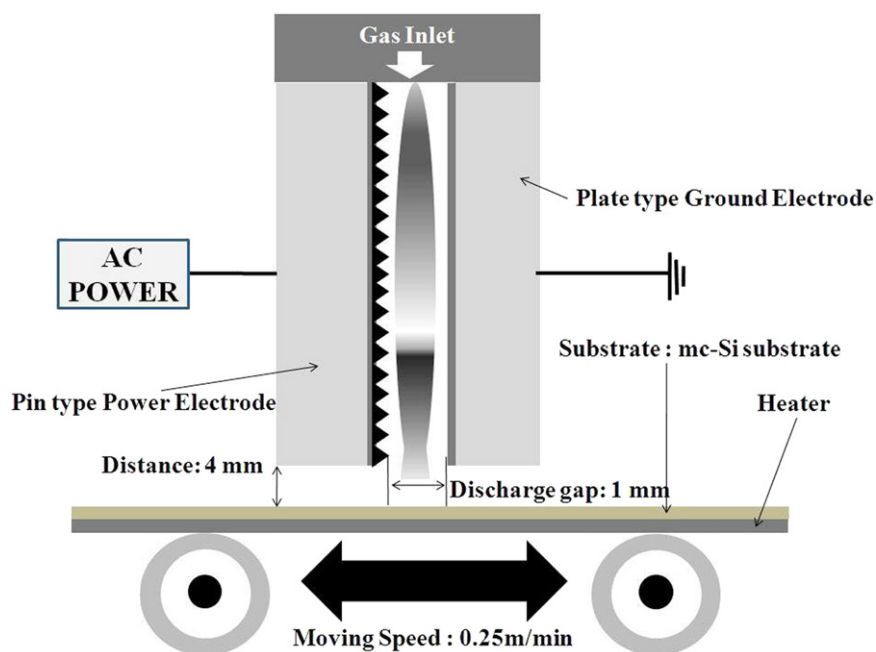


**Figure 1.** Schematic diagram of the remote-type atmospheric-pressure discharge system (pin-to-plate DBD) used in the experiment.

undesirable, because of the large amount of chemicals used. Therefore, many researchers have investigated dry processing methods that use low-pressure reactive ion etching (RIE), either with a mask in order to achieve large and regular features or else without a mask in order to produce a much smaller and more random wave-type texture [6, 7]. However, RIE requires a vacuum system, which makes it very expensive, in addition to the problems related to its throughput. Furthermore, in the case of RIE, the ion bombardment by the reactive ions can damage the mc-Si surface during the etching and texturing processes.

Atmospheric-pressure plasmas have been investigated as a possible replacement for low-pressure plasma processing in a number of areas, including semiconductor and flat panel display processing. Currently, using the typical, inefficient atmospheric-pressure plasmas composed of a dielectric barrier discharge (DBD) is known to be more expensive than wet etching, due to the large energy used for the discharge and the undesirable amount of gases required for processing. However, if a more efficient system were developed, the use of an atmospheric-pressure plasma would not only decrease the processing cost, but also increase the product throughput by enabling an in-line system to be employed. Consequently, this technique has been investigated for surface treatment, etching and thin film deposition [8–10]. In this study, we used a more efficient atmospheric-pressure plasma in an etching application to remove the saw damage and texture the mc-Si surface for use in a solar cell. To produce the atmospheric-pressure plasma, we used a modified DBD called a ‘remote-type pin-to-plate DBD’ to increase the processing rate by increasing the plasma density [11, 20] without damaging the substrate surface. We investigated the effects of adding gases, such as  $\text{NF}_3$  and  $\text{O}_2$ , to the  $\text{N}_2$ -based atmospheric-pressure plasma on the etching and texturing characteristics of mc-Si.

## 2. Experimental setup

Figure 1 shows a schematic diagram of the remote plasma-type pin-to-plate DBD system used in the experiment. The discharge source was composed of a multi-pin power electrode and a blank ground electrode located vertically above the substrate. The electrodes were made of aluminium and each had a size of  $50 \times 300 \text{ mm}^2$ . The power electrode was machined to have multi-pins with a pyramid shape, as shown in figure 1, while the ground electrode had just a flat surface. Both electrodes were coated with  $300 \mu\text{m}$  thick alumina to function as a dielectric layer in the DBD system. The discharge gap, which is the distance between the power electrode and the ground electrode, was fixed at 1 mm. The power electrode was connected to an alternating current (ac) power supply with a frequency of 30 kHz and a maximum power of 4 kW. For this study, the input voltage to the power electrode was kept at 8 kV (rms voltage).  $\text{N}_2$  gas was used as the discharge gas, while  $\text{NF}_3$  and  $\text{O}_2$  were used as reactive gases. The mc-Si wafer substrate was fed below the remote-type DBD source at a speed of  $0.25 \text{ m min}^{-1}$ . The substrate was heated to  $120^\circ\text{C}$ , and the distance between the substrate and the remote-type DBD source module was maintained at 4 mm.

We estimated the mc-Si etching rate by measuring the etching depth using a step profilometer (TENCOR, alpha-step 500). To measure the etch rate (nm/scan), the mc-Si etch depth was measured after 15–20 scans and the etch rate was estimated by dividing the etch depth by the number of etch scans. We also measured the optical emission intensities of the species emitted from the plasma using an optical emission spectroscope (OES, PCM 420 SC-Technology), in order to detect radicals or activated species in the plasma. Chemical information about the textured mc-Si surface was obtained using x-ray photoelectron spectroscopy (XPS, Thermo VG Sigma Probe). The reflectance of the textured mc-Si was

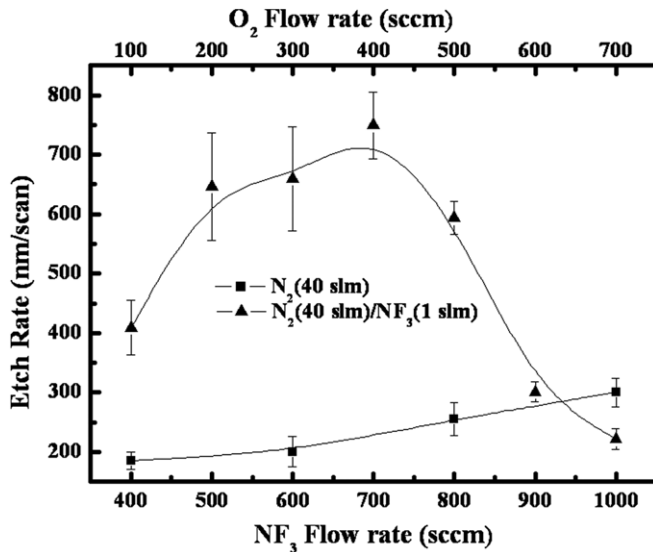


**Figure 2.** Effect of additive gas flow rates ( $\text{NF}_3$  (0.4–1 slm) to  $\text{N}_2$  (40 slm) and  $\text{O}_2$  (0–1 slm) to  $\text{N}_2$  (40 slm)/ $\text{NF}_3$  (1 slm)) on the mc-Si etch rate. The input voltage was 8 kV and the frequency was 30 kHz. The substrate was moving at a speed of  $0.25 \text{ m min}^{-1}$  and the substrate temperature was maintained at  $120^\circ\text{C}$ .

measured by a UV-Vis spectrophotometer (UV-Vis, UV-3600 Shimadzu).

### 3. Results and discussion

Figure 2 shows the effect of  $\text{NF}_3$  and  $\text{O}_2$  on the etch rate (nm/scan) of mc-Si, measured as functions of the amount of  $\text{NF}_3$  added to  $\text{N}_2$  (40 slm) and the amount of  $\text{O}_2$  added to  $\text{N}_2$  (40 slm)/ $\text{NF}_3$  (1 slm) for the modified remote-type pin-to-plate DBD. An ac voltage of 8 kV rms at 30 kHz was applied to the power electrode and the ground electrode was heated to  $120^\circ\text{C}$ . As shown in the figure, increasing the  $\text{NF}_3$  flow rate increased the mc-Si etch rate almost linearly from 185 nm/scan at 400 sccm of  $\text{NF}_3$  to 300 nm/scan at 1 slm of  $\text{NF}_3$ . Raising the  $\text{NF}_3$  flow rate above 1 slm also increased the etch rate of mc-Si, and the increase in the mc-Si etch rate with increasing  $\text{NF}_3$  flow rate is believed to be related to the increase in the amount of  $\text{F}^-$  radicals in the plasma, forming volatile  $\text{SiF}_x$  with the mc-Si. While maintaining the  $\text{NF}_3$  flow rate at 1 slm,  $\text{O}_2$  was added and, as shown in the figure, the addition of  $\text{O}_2$  to  $\text{N}_2$  (40 slm)/ $\text{NF}_3$  (1 slm) increased the mc-Si etch rate from 409 nm/scan at 100 sccm of  $\text{O}_2$  to 750 nm/scan at 400 sccm of  $\text{O}_2$ . Therefore, the addition of 400 sccm  $\text{O}_2$  to  $\text{N}_2$  (40 slm)/ $\text{NF}_3$  (1 slm) increased the mc-Si etch rate by a factor of nearly 2.5. However, increasing the  $\text{O}_2$  flow rate further to 800 sccm caused the mc-Si etch rate to decrease.

Using optical emission spectroscopy, we investigated the variation in the density of radicals with the  $\text{O}_2$  flow rate in the DBD area. Figure 3 shows the relative optical emission intensities of F ( $I_{\text{F}}/I_{\text{Ar}}$ ), O ( $I_{\text{O}}/I_{\text{Ar}}$ ) and NO ( $I_{\text{NO}}/I_{\text{Ar}}$ ) measured as a function of the flow rate of  $\text{O}_2$  added to  $\text{N}_2$  (40 slm)/ $\text{NF}_3$  (1 slm). For the relative measurement, Ar actinometry was used by adding 1 slm of Ar to the discharge gas and measuring the ratio of the radical intensities to the

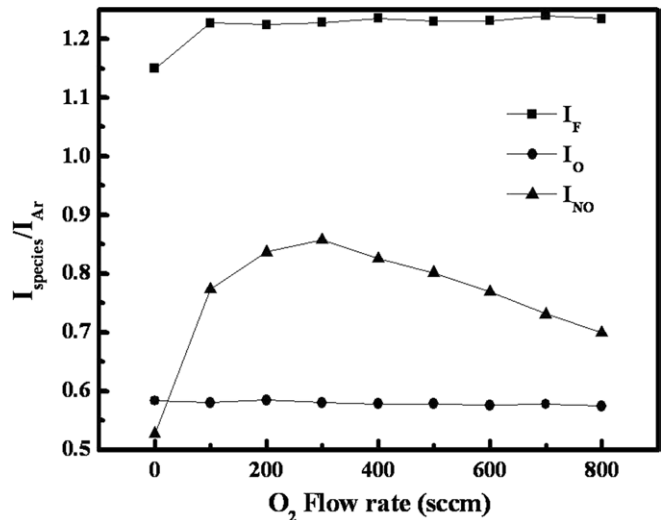


**Figure 3.** Relative optical emission intensities measured as a function of oxygen gas flow rate in  $\text{N}_2$  (40 slm)/ $\text{NF}_3$  (1 slm) gas mixture.  $I_{\text{F}}/I_{\text{Ar}}$  and  $I_{\text{NO}}/I_{\text{Ar}}$  are shown. Ar gas (1 slm) was added for the actinometry measurements. The input voltage was 8 kV and the frequency was 30 kHz.

intensity of Ar [12]. The optical emission intensities observed at 750.4 nm, 703.7 nm and 844.6 nm were assigned as the atomic emission peaks of Ar, F and O, respectively. The optical emission intensity of NO was in the range from 200 to 300 nm and, for our measurement, we assigned the highest peak at 241.3 nm as the NO peak [12–14]. As shown in the figure, the addition of a small amount of oxygen to the  $\text{N}_2$ / $\text{NF}_3$  flow increased the relative F intensity, and increasing the oxygen flow rate slowly increased the F intensity. The O intensity did not vary significantly with the oxygen gas flow rate in the  $\text{N}_2$ / $\text{NF}_3$  gas mixture. The NO intensity increased as the oxygen flow rate increased up to 300 sccm and then began to decrease. The lack of any significant change in the O intensity with increasing oxygen flow rate in the figure appears to be related to the consumption of O by the formation of NO and possibly  $\text{O}_3$  in the plasma. The initial increase in the NO intensity with increasing oxygen flow rate may be due to the recombination between the N from  $\text{N}_2$  and the O from  $\text{O}_2$ , but it has also been reported that, in plasmas generated from a gas mixture of  $\text{NF}_3$  and  $\text{O}_2$ ,  $\text{NO}_x$  is formed more easily than NF or  $\text{NF}_2$ , so the partial NO intensity observed in the figure is believed to result from the recombination of N from  $\text{NF}_3$  and O from  $\text{O}_2$  [15]. Given that NO is formed from  $\text{NF}_3$  and  $\text{O}_2$ , an increase in the relative intensity of F is to be expected with the addition of and increase in the flow rate of oxygen. The decrease in the amount of NO when the oxygen flow rate exceeds 300 sccm is believed to be related to the increased electron attachment to oxygen with increasing oxygen flow rate, which decreases the electron density in the plasma [11]. In fact, if too much oxygen flow is introduced, a filamentary discharge is observed.

As shown in figure 3, the addition of and increase in the flow rate of oxygen in the  $\text{N}_2$ / $\text{NF}_3$  gas can increase the F atomic density in the plasma, which in turn can increase the mc-Si etch rate. However, increasing the oxygen flow rate in the  $\text{N}_2$ / $\text{NF}_3$  gas mixture can also oxidize the silicon surface

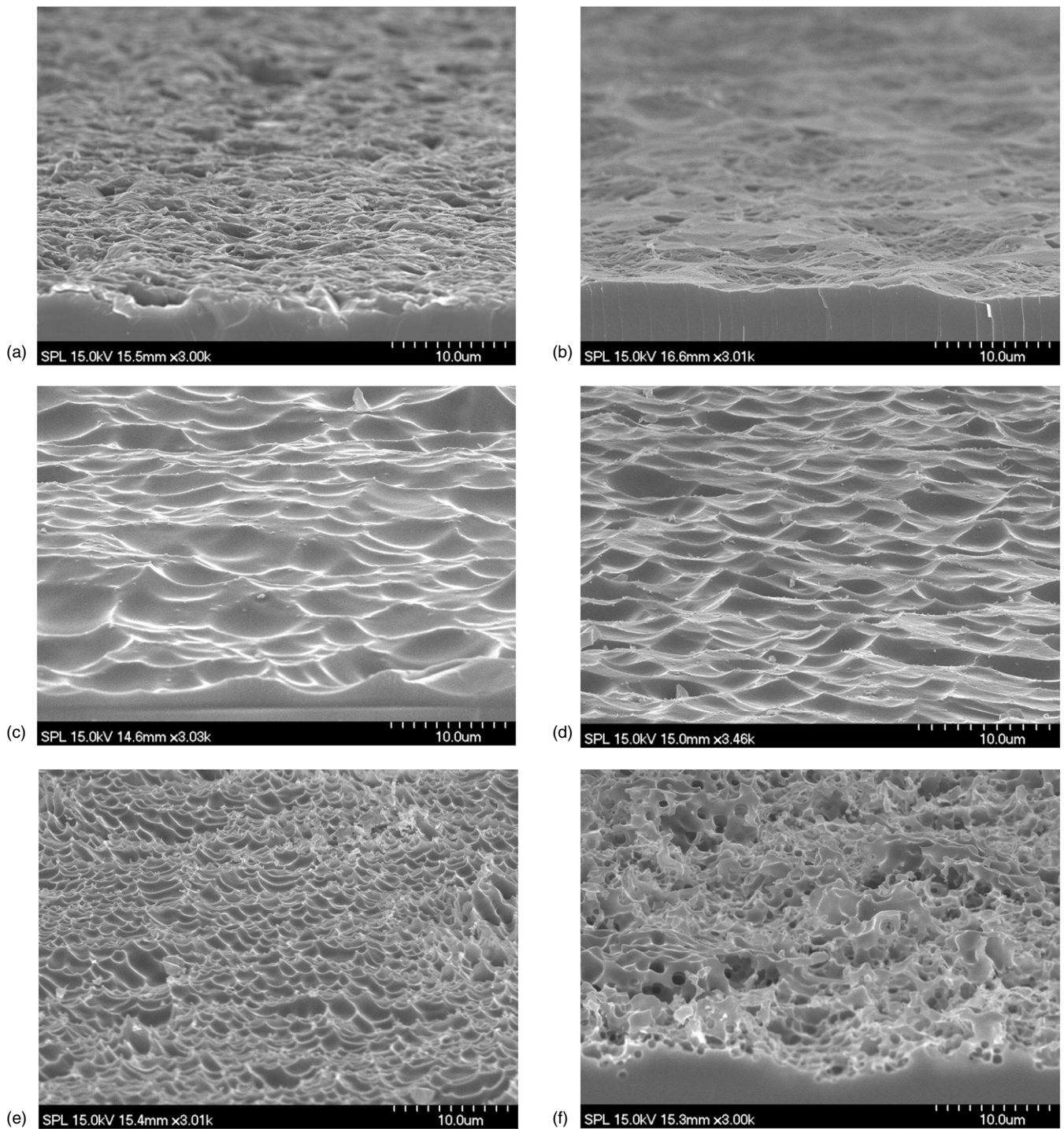


**Figure 4.** SEM images of various textured mc-Si surfaces as a function of the additive  $O_2$  gas flow rate in  $N_2$  (40 slm)/ $NF_3$  (1000 sccm): (a) as-received (sliced mc-Si), (b) without  $O_2$ , (c)  $O_2$ : 200 sccm, (d)  $O_2$ : 400 sccm, (e)  $O_2$ : 600 sccm, (f)  $O_2$ : 800 sccm. The input voltage was 8 kV and the frequency was 30 kHz. The substrate was moving at a speed of  $0.25 \text{ m min}^{-1}$  and the temperature of the substrate was fixed at  $120^\circ\text{C}$ . The mc-Si etch depth was about  $6 \mu\text{m}$ .

through oxygen-related reactive species such as O, NO and  $O_3$ , which would decrease the mc-Si etch rate. Therefore, the initial increase in the mc-Si etch rate observed with the initial increase in the oxygen flow rate in figure 2 is believed to be related to the increase in the amount of F (radicals?) in the plasma, while the decrease in the mc-Si etch rate at higher oxygen flow rates is related to the oxidation of the mc-Si surface.

We used SEM to observe the mc-Si surface morphology, in order to investigate the change in the surface texturing with the oxygen flow after etching about  $5\text{--}10 \mu\text{m}$  from the mc-Si surface (which varied with the  $O_2$  flow rate). Figures 4(a)–(f) show the SEM micrographs taken before and after etching at various oxygen flow rates: (a) as-received, (b) 0 sccm, (c) 200 sccm, (d) 400 sccm, (e) 600 sccm and (f) 800 sccm added to  $N_2$  (40 slm)/ $NF_3$  (1000 sccm). As shown in the figures,

the as-received mc-Si showed a certain surface roughness due to the slicing of the mc-Si ingot. When the mc-Si was etched without the addition of oxygen, a relatively flat mc-Si surface was observed, because of the smoothing induced by the isotropic etching by the remote-type  $N_2/NF_3$  plasma. That is, when no oxygen was added, due to the dissociation of  $NF_3$  ( $NF_3 \rightarrow NF_x + F_x$ ), reactive species such as F are diffused onto all of the exposed mc-Si surface and react with silicon to form volatile  $SiF_4$ . However, as the rate of the oxygen flow added to the  $N_2/NF_3$  gas mixture was increased, the surface became rougher. The surface texturing morphology was of the wave type up to an  $O_2$  flow rate of 600 sccm; this is the morphology required to decrease the reflection of light from the silicon surface. However, when 800 sccm of  $O_2$  was added, even though the surface roughness was higher, its morphology became very irregular and exhibited an undesirable shape for a solar cell; the mc-Si etch rate was also decreased significantly. This change in the surface texturing morphology with increasing rate of oxygen flow is believed to be related to the micromasking effect.

During the etching in  $N_2/NF_3$  with oxygen flow, the mc-Si surface is locally oxidized by oxidizing species such as O, NO and  $O_3$ , while simultaneously being etched by F. In fact, certain areas of the mc-Si surface can be significantly more oxidized than others, possibly due to the defects present, such as cracks, voids and grain boundaries. When there is no oxygen or the oxygen flow rate is low, the local surface oxidation rate is slow and, therefore, most of the surface is etched more or less evenly by F and generally remains flat. However, as the amount of oxygen in the gas mixture is increased, the local surface oxidation rate is increased. At the same time, due to the significant differences in the etch rates between the locally oxidized surface and the clean mc-Si surface in the F-based plasma, the surface morphology becomes more wave shaped. Therefore, in specific surface areas, the micromasking effect, which acts as a mask for etching, is increased with increasing oxygen flow rate, and a wave-shaped etching profile is obtained. When the oxygen flow rate is too high, the resulting severe micromasking effect leads to a very rough surface, as shown in figure 4(d).

To investigate the possibility of the micromasking of mc-Si by surface oxidation, we used XPS to examine the mc-Si surfaces etched at various rates of oxygen flow in  $N_2/NF_3$ . Figures 5(a) and (b) show the O 1s and Si 2p photoemission intensity peaks, respectively, measured from the etched silicon surfaces as a function of the oxygen flow rate. As shown in figure 5(a), for the O 1s peak, when no oxygen was added, a small oxygen peak is observed at 533 eV; this peak is related to the Si– $O_2$  bonding of the native oxide, which may be caused by the exposure of the etched mc-Si surface to air before the measurement [16]. As the oxygen flow rate is increased, the O 1s peak intensity increases due to the increased surface oxidation. The peak location is also shifted to lower binding energies, indicating the formation of Si–O–N on the silicon surface; it is known that increasing the Si–O–N bonding shifts the O 1s bonding peak to a lower binding energy [17, 18]. Similarly, for the Si 2p photoemission peak, when no oxygen was added, the Si–Si bonding peak was observed at 99.1 eV in

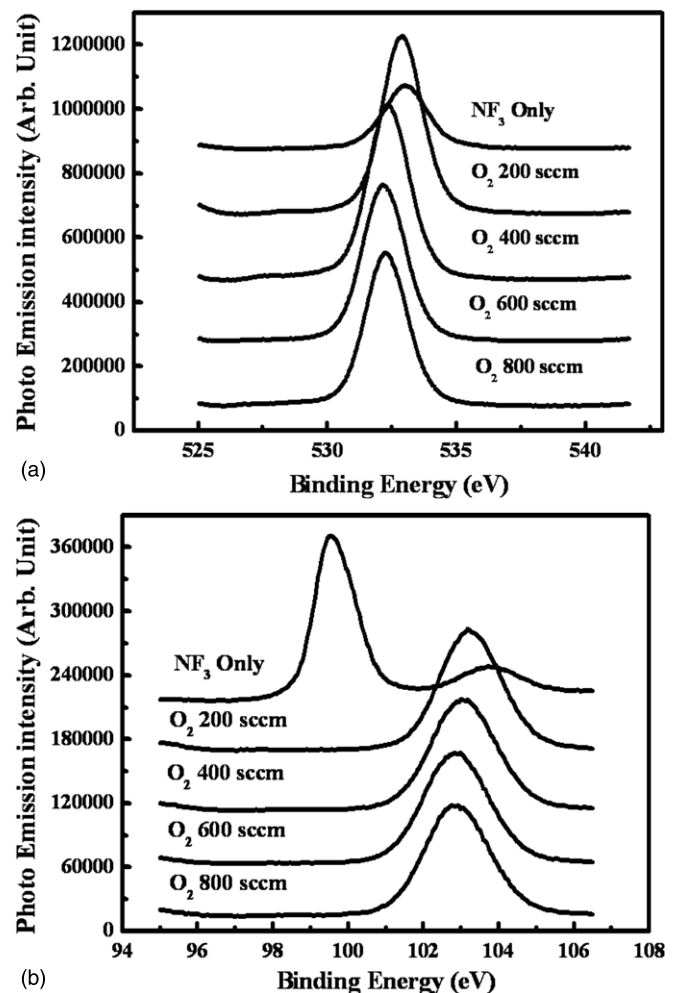


**Figure 5.** Narrow scan XPS spectra of (a) O 1s and (b) Si 2p for the mc-Si surface after etching as a function of additive  $O_2$  gas flow rate in  $N_2$  (40 slm)/ $NF_3$  (1000 sccm). The etch condition is the same as shown in figure 4.

addition to a very small Si–O bonding peak at 103.3 eV related to the native silicon oxide [16]. However, with the addition of and increase in the flow rate of oxygen in the  $N_2/NF_3$  gas mixture, it was possible to observe an increase in the peak intensity related to Si–O bonding, indicating the presence of surface oxidation. In addition, the Si–O bonding peak intensity was shifted to a lower bonding energy related to Si–N (102 eV), because increasing the oxygen flow rate led to the formation of Si–O–N bonds [19]. Therefore, from the above results, we can conclude that the increase in the surface roughness with increasing oxygen flow rate is related to micromasking caused by local surface oxidation, forming species such as Si–O and Si–O–N.

With the mc-Si wafers having various surface morphologies obtained from the different oxygen flow rates shown in figure 4, we measured the optical reflectance. The results are shown in figure 6 and, as a reference, the reflectance of the as-received mc-Si wafer is also included. As seen in the figure, when the mc-Si was etched without adding oxygen, the smoothing effect caused the reflectance in the visible range to increase from 30–40% to 30–60%. As the oxygen flow rate in the  $N_2/NF_3$  gas mixture was increased, the reflectance

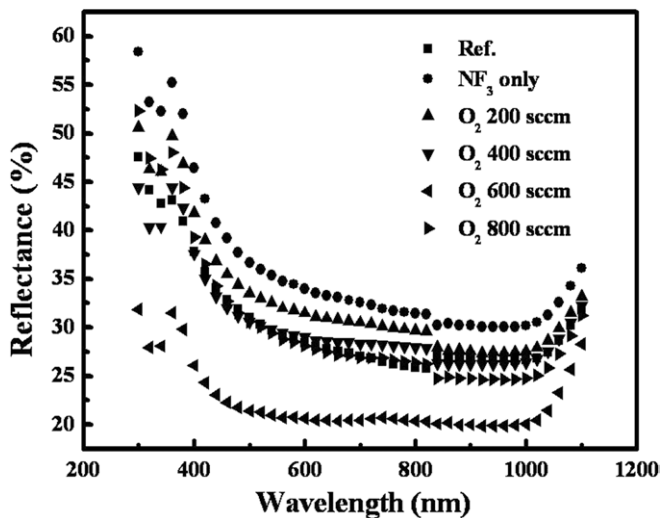


**Figure 6.** Reflectance of the textured mc-Si as a function of the additive  $O_2$  gas flow rate in  $N_2$  (40 slm)/ $NF_3$  (1000 sccm). The etch condition is the same as shown in figure 4.

decreased, because of the increase in the surface roughness; the lowest reflectance of 20–30% in the visible range was achieved at an oxygen flow rate of 600 sccm. Even though the surface roughness was higher at an oxygen flow rate of 800 sccm than that at 600 sccm, the reflectance was higher, indicating that the optimal surface morphology for low reflectance is the deep wave shape, not the irregular shape.

#### 4. Conclusions

We investigated maskless atmospheric-pressure plasma texturing and a high-speed etching process for mc-Si using a pin-to-plate-type DBD with varying rates of oxygen flow added to the  $N_2$ (40 slm)/ $NF_3$  (1 slm) gas mixture. When the mc-Si wafer was etched in  $N_2/NF_3$ , increasing the  $NF_3$  flow rate increased the mc-Si etch rate, causing the etched mc-Si surface to be smooth. When oxygen was added to  $N_2/NF_3$ , the mc-Si etch rate was further increased due to the increase in the amount of F caused by the dissociation of  $NF_3$ , which was caused by the combination of N with O to form NO; the etch rate increased as the oxygen flow rate increased up to 400 sccm. Increasing the oxygen flow rate beyond this point, however, decreased the mc-Si etch rate, because of surface oxidation. At the same time, surface oxidation to form Si–O and Si–O–N bonds, caused by the addition of oxygen to  $N_2/NF_3$ , increased the surface roughness due to the appearance of micromasking on the mc-Si surface. The optimum surface roughness, having the deep wave-type texturing required for mc-Si solar cells, could be obtained by the addition of 600 sccm  $O_2$ ; at that flow rate, the minimum reflectance of 20–30% in the visible wavelength range was obtained at an etch rate of 300 nm/scan (0.25 m/scan). Therefore, even though a reflectivity of less than 15% is

currently obtained by conventional wet processing, it is believed that, after further improvement, atmospheric-pressure plasma processing could be applied to the etching and texturing of mc-Si for high efficiency mc-silicon solar cells, instead of conventional wet processing, due to its various advantages, such as its low environmental impact and easier in-line processing.

#### Acknowledgments

This work was carried out through the Direct Nano Patterning Project supported by the Ministry of Knowledge Economy (MKE) under the National Strategic Technology Programme. This work was also supported by the Korea Industrial Technology Foundation (KOTEF) through the Human Resource Training Project for Strategic Technology.

#### References

- [1] Zaho J, Wang A and Green M A 1998 *Appl. Phys. Lett.* **73** 1991
- [2] Kim J M and Kim Y K 2005 *J. Electrochem. Soc.* **152** G189
- [3] Ruby D S, Zaidi S, Narayanan S, Yamanaka S and Balanga R 2005 *J. Sol. Energy Eng.* **127** 146
- [4] Schultz O, Emanuel G, Glunz S W and Wileke G P 2003 *3rd World Conf. on Photovoltaic Energy Conversion (Osaka, Japan, May 2003)*
- [5] Panek P, Lipinski M and Dutkiewicz J 2005 *J. Mater. Sci.* **40** 1459
- [6] Macdonald D H, Cuevas A, Kerr M J, Samundsett C, Ruby D, Winderbaum S and Leo A 2004 *Sol. Energy* **76** 277
- [7] Ruby D S, Zaidi S H, Roy M and Narayanan M 1999 *9th Workshop on Crystalline-silicon Cell Materials and Processes (Breckenridge, CO, USA, August 1999)*
- [8] Okazaki S, Kogoma M, Uehara M and Kimura Y 1993 *J. Phys. D: Appl. Phys.* **26** 889
- [9] Yokoyama T, Kogoma M, Kanazawa S, Moriawaki T and Okazaki S 1990 *J. Phys. D: Appl. Phys.* **23** 374
- [10] Yokoyama T, Kogoma M, Moriawaki T and Okazaki S 1990 *J. Phys. D: Appl. Phys.* **23** 1125
- [11] Lee Y H, Kyung S J, Jeong C H and Yeom G Y 2004 *Japan. J. Appl. Phys.* **44** L78
- [12] Coburn J W and Chen M 1980 *J. Appl. Phys.* **51** 3134
- [13] Donnelly V M, Malyshev M V, Schabel M, Kornblit A, Tai W, Herman I P and Fuller N C M 2002 *Plasma Source Sci. Technol.* **11** A26
- [14] Massines F, Segur P, Gherardi N, Khamphan C and Ricard A 2003 *Surf. Coat. Technol.* **174–175** 8
- [15] Nagata A, Ichihashi H, Kusunoki Y and Horiike Y 1989 *Japan. J. Appl. Phys.* **28** 2368
- [16] Moulder J F, Stickle W F, Sobol P E and Bombardier K D 1992 *Handbook of X-ray Photoelectron Spectroscopy* (Minnesota: Perkin-Elmer Corporation Physical Electronics Division)
- [17] Matsuo P J, Kastenmeier B E E and Oehrlein G A 1999 *J. Vac. Sci. Technol. A* **17** 2431
- [18] Poon M C, Kok C W, Wong H and Chan P J 2004 *Thin Solid Films* **462–463** 42
- [19] Wong C K, Wong H, Filip V and Chung P S 2007 *Japan. J. Appl. Phys.* **46** 3202
- [20] Lee Y H and Yeom G Y 2005 *J. Korea Phys. Soc.* **47** 74